

# Arctic soil CO<sub>2</sub> release during freeze-thaw cycles modulated by silicon and calcium

## Authors

*Jörg Schaller<sup>1\*</sup>, Peter Stimmler<sup>1</sup>, Mathias Göckede<sup>2</sup>, Jürgen Augustin<sup>1</sup>, Fabrice Lacroix<sup>2, 3</sup> and Mathias Hoffmann<sup>1</sup>*

## Affiliations

<sup>1</sup> Leibniz Center for Agricultural Landscape Research (ZALF), 15374 Müncheberg, Germany

<sup>2</sup> Max Planck Institute for Biogeochemistry, Jena, Germany

<sup>3</sup> Climate and Environmental Physics, University of Bern, Bern, Switzerland

\*Corresponding author Email: Joerg.Schaller@zalf.de

1 **Arctic soil CO<sub>2</sub> release during freeze-thaw cycles modulated by silicon and**  
2 **calcium**

3

4 **Authors**

5 *Jörg Schaller<sup>1\*</sup>, Peter Stimmler<sup>1</sup>, Mathias Göckede<sup>2</sup>, Jürgen Augustin<sup>1</sup>, Fabrice Lacroix<sup>2,3</sup>*  
6 *and Mathias Hoffmann<sup>1</sup>*

7

8 **Affiliations**

9 <sup>1</sup> Leibniz Center for Agricultural Landscape Research (ZALF), 15374 Müncheberg, Germany

10 <sup>2</sup> Max Planck Institute for Biogeochemistry, Jena, Germany

11 <sup>3</sup> Climate and Environmental Physics, University of Bern, Bern, Switzerland

12

13 \*Corresponding author Email: Joerg.Schaller@zalf.de

14

15

17 **Abstract**

18 Arctic soils are the largest pool of soil organic carbon worldwide. Temperatures in the Arctic  
19 have risen faster than the global average during the last decades, decreasing annual freezing  
20 days and increasing the number of freeze-thaw cycles (temperature oscillations passing  
21 through zero degrees) per year as the temperature is expected to fluctuate more around 0°C.  
22 At the same time, proceeding deepening of seasonal thaw may increase silicon (Si) and  
23 calcium (Ca) concentrations in the active layer of Arctic soils as the concentrations in the  
24 thawing permafrost layer might be higher depending on location. We analyzed the importance  
25 of freeze-thaw cycles for Arctic soil CO<sub>2</sub> fluxes. Furthermore, we tested how Si (mobilizing  
26 organic C) and Ca (immobilizing organic C) interfere with the soil CO<sub>2</sub> fluxes in the context  
27 of freeze-thaw cycles. Our results show that with each freeze-thaw cycle the CO<sub>2</sub> fluxes from  
28 the Arctic soils decreased. Our data revealed a considerable CO<sub>2</sub> emission below 0°C. We  
29 also show that pronounced differences emerge in Arctic soil CO<sub>2</sub> fluxes with Si increasing  
30 and Ca decreasing CO<sub>2</sub> fluxes. Furthermore, we show that both Si and Ca concentrations in  
31 Arctic soils are central controls on Arctic soil CO<sub>2</sub> release, with Si increasing Arctic soil CO<sub>2</sub>  
32 release especially when temperatures are just below 0°C. Our findings could provide an  
33 important constraint on soil CO<sub>2</sub> emissions upon soil thaw, as well as on the greenhouse gas  
34 budget of high latitudes. Thus we call for work improving understanding of freeze-thaw  
35 cycles as well as the effect of Ca and Si on carbon fluxes, as well as for increased  
36 consideration of those factors in wide-scale assessments of carbon fluxes in the high latitudes.

37

38

39 **Keywords:** amorphous silica; Arctic soil; calcium; climate change; greenhouse gas release;  
40 nutrient; soil respiration

42

## 43 **1 Introduction**

44 There is large evidence from a variety of biomes covering temperate to higher  
45 latitudes that freeze-thaw cycles can strongly influence soil respiration (Kurganova et al.,  
46 2007; Ouyang et al., 2015; Skogland et al., 1988). While respiration is usually very low  
47 during the freeze phase, a brief strong CO<sub>2</sub> pulse often occurs during thaw, followed by a  
48 rapid decline in CO<sub>2</sub> release afterwards (Kim et al., 2012; Saprnov, 2021; Zhang et al.,  
49 2021). Such strong CO<sub>2</sub> release after thawing is likely to be important for soils which store  
50 large amounts of organic carbon vulnerable for microbial respiration (Skogland et al., 1988).  
51 Suchs soil with large amounts of vulnerable organic carbon are the soils in the Arctic  
52 (Hugelius et al., 2014).

53 Arctic soils are the largest pool of soil organic carbon (C) worldwide (Strauss et al.  
54 2017). Approximately, 1300 Tg of organic C are stored within the first 3 m (Hugelius et al.  
55 2014). Temperatures in the high latitudes have risen faster as the global average in the last  
56 decades, decreasing annual freezing days (Henry, 2007; Stocker et al., 2014). Thawing of  
57 permafrost in Arctic soils due to climate warming exposes large amounts of organic C  
58 vulnerable to microbial degradation (Heslop et al., 2019; Mueller et al., 2015; Treat et al.,  
59 2021), thus potentially increasing C emissions of Arctic terrestrial systems, which potentially  
60 warms the climate through the greenhouse effect. Accordingly, CO<sub>2</sub> released from Arctic soils  
61 to the atmosphere as a result of soil organic matter degradation by microorganisms  
62 (heterotrophic respiration) could strongly impact future climate change, and should be  
63 considered for defining current climate goals (Anderson et al., 2016; Canadell et al., 2021;  
64 Schuur et al., 2015).

65 The few studies that have been conducted on Arctic soils in this regard mostly follow  
66 the picture of experiments from other biomes showing a strong CO<sub>2</sub> release after each thaw

67 event (Kim et al., 2012; Ludwig et al., 2006; Saproinov, 2021; Schimel and Clein, 1996; Wang  
68 et al., 2014).

69 In deeper Arctic soils, which were previously permanently frozen, increased  
70 temperatures will firstly expose permanently frozen parts of the soil to freeze thaw cycles and  
71 secondly increase the number of freeze-thaw cycles per year (oscillation around 0°C), as the  
72 temperature is fluctuating more around 0°C (Henry, 2008). Each thawing is accompanied by a  
73 strong increase in the concentration and quantities of both microbial degradable organic  
74 compounds and a number of other elements in the soil solution (Loiko et al., 2017; Payandi-  
75 Rolland et al., 2020). Such increase in element availability by thawing may be particularly  
76 important for silicon (Si) and calcium (Ca) altering the concentrations of both elements in the  
77 soil active layer (Alfredsson et al., 2016; Stimmler et al., in revision; Walker et al., 2001).  
78 Both elements may strongly interfere with soil organic C mineralization and soil CO<sub>2</sub> release  
79 (Schaller et al., 2019). Ca is known to bind organic C by cation bridging in Arctic soils  
80 (Whittinghill and Hobbie, 2012), while Si mobilizes organic C due to competition for binding  
81 at the surface of soil particles (Hömborg et al., 2020; Reithmaier et al., 2017; Schaller et al.,  
82 2019). These effects on organic C mobility have been reported to substantially affect the soil  
83 CO<sub>2</sub> release in incubation experiments of high-Arctic soils (Schaller et al., 2019; Stimmler et  
84 al., 2022). Consequently, we expect that Si increases and Ca decreases Arctic soil C fluxes.

85 However, up to now, no study analyzed the importance of freeze-thaw cycles (potentially  
86 mobilizing organic C) while considering effects caused by Si (mobilizing organic C) or Ca  
87 (immobilizing organic C) for Arctic soil CO<sub>2</sub> release especially under freezing conditions and  
88 upon thaw. In this study, we hypothesize that (i) every freeze-thaw cycle will lead to a  
89 consistent pronounced CO<sub>2</sub> release after thaw and (ii) Si is positively and Ca negatively  
90 related to Arctic soil CO<sub>2</sub> emissions. To investigate this, we used controlled laboratory  
91 incubation experiments to test the combination of freeze-thaw cycles, as well as Si and Ca for

92 Arctic soil CO<sub>2</sub> release. To make the freeze-thaw experiments comparable with natural  
93 conditions we adapted the freeze-thaw regime to the natural freeze-thaw cycle of the Arctic  
94 soils to make sure that freezing as well as thawing periods allowed the soil microbes to adapt.

95

96

## 97 **2 Materials and Methods**

### 98 *2.1 Soil material used for experiments*

99 The soil used for the present study was taken from a wet tussock tundra ecosystem near  
100 Chersky, Northeast Siberia, Russia (68,61586°N; -161,35228°E), underlain by continuous  
101 permafrost (Göckede et al., 2017; Göckede et al., 2019). The soil, which was sampled from  
102 the mineral active layer from 50 to 60 cm depth, was gently crushed in frozen state using a  
103 steel mortar in a first processing step. The frozen material was split and sieved under frozen  
104 conditions through a two mm sieve until all particles passed through the sieve. The soil had an  
105 amorphous Si content of 3mg g<sup>-1</sup>, and Mehlich(III) extractable concentrations of 0.08mg g<sup>-1</sup>  
106 for Si, and 0.6mg g<sup>-1</sup> for Ca (Stimmler et al., in revision). The soil samples were completely  
107 saturated with water during the whole experiment.

108

### 109 *2.2 Experimental design and analysis*

110 To make the freeze-thaw experiments comparable with natural conditions, we adapted the  
111 laboratory freeze-thaw regime to the natural freeze-thaw cycle as observed within the Arctic  
112 soils at the sampling site near Chersky. For this, the soils were incubated at +5°C until the  
113 CO<sub>2</sub> efflux was at equilibrium (Fig. 1). Afterwards, the soil temperature was decreased to  
114 +1°C within two days. The temperature of +1°C was held for two days. and afterwards the  
115 temperature was decreased to -1°C and held for two days, again. Thereafter, the temperature

116 was decreased to  $-9^{\circ}\text{C}$  (Fig. 1). This temperature profile allows microbes to adapt to the  
117 temperatures is analog to field conditions. Such adaptation is important as microbes are  
118 sensitive toward freezing at too fast rates (Lipson et al., 2000). The chosen moderate  
119 temperature gradients prevent lysis as shown for such conditions before (Grogan et al., 2004).  
120 Linear extrapolated  $\text{CO}_2$  flux rates, initially measured during  $-1^{\circ}\text{C}$ , were used in this study as  
121 a conservative estimate for  $\text{CO}_2$  efflux during freeze periods.

122

### 123 ***2.3 Measurements and data analysis***

124 We incubated four different sample treatments, namely a natural soil (control), and three  
125 further treatments with added silicon (+Si), added calcium (+Ca), and both added silicon and  
126 calcium (+Si+Ca).  $\text{CO}_2$  and  $\text{CH}_4$  fluxes from the samples were analyzed for three thaw  
127 periods (Table 1). For each treatment, four replicates of 20g each were incubated in parallel  
128 using the incubation system described in detail by Rillig et al. (2021). The used incubation  
129 system works in a flow-through, steady-state mode corresponding to Livingston and  
130 Hutchinson (1995). It contains 16 airtight, cylindrical incubation vessels (50 mL PE centrifuge  
131 vials), for the samples to be incubated, and a control channel through which ambient air  
132 passes the incubation vessels directly from the pressure vessel to the gas analyzer (Picarro  
133 G2508; PICARRO, INC., Santa Clara, USA). Ambient air flows was continuously through  
134 the headspace of all incubation vessels via channels connecting the pressure vessel and the  
135 gas analyzer directly, using a multiplexer and a special circular channel. Air was circulated  
136 between the incubation unit headspace and the CRDS analyzer at  $250\text{ mL min}^{-1}$  using a low-  
137 leak diaphragm pump (A0702, Picarro, Santa Clara, CA, USA). To increase the sensitivity of  
138 the incubation system, flow rate and measurement time per channel were adjusted according  
139 to the expected  $\text{CO}_2$  flux rate. The temperature was controlled in the incubation vessels by  
140 means of a climate chamber. During the thawing phases, the samples were weighed several

141 times to compensate for possible soil water losses. CO<sub>2</sub> fluxes were calculated from the  
142 measured CO<sub>2</sub> gas concentration in the respective channel, and the temporally corresponding  
143 concentration in the control channel according to Equation 1:

$$144 \quad F = \frac{(M * \rho * V * (\Delta c))}{(C * R * t * T)}$$

145 where F is the flux rate ( $\mu\text{g CO}_2\text{-C core}^{-1} \text{ h}^{-1}$ ), M is the molar mass of CO<sub>2</sub>,  $\rho$  the atmospheric  
146 pressure (Pa), V is the air flow rate into the headspace and the channels ( $\text{m}^3 \text{ h}^{-1}$ ),  $\Delta c$  is the  
147 difference of CO<sub>2</sub> concentrations [mol] between outlet of a specific vessel and the  
148 corresponding, linear interpolated control channel CO<sub>2</sub> concentration, C is the soil sample  
149 area ( $\text{m}^2$ ), R the gas constant ( $\text{m}^3 \text{ Pa K}^{-1} \text{ mol}^{-1}$ ), t is the time over which the concentration  
150 change was observed, and T the incubation temperature (K).

151 Fluxes were calculated using an R script. Influence of diurnal cycles in measured ambient air  
152 within the control channel on calculated CO<sub>2</sub> fluxes was minimized by linear interpolation of  
153 CO<sub>2</sub> concentrations measured for the control channel, rather than using adjacent control  
154 channel CO<sub>2</sub> concentration measurements only. To avoid bias caused by measurements on the  
155 previous channel, only values determined in the last minute of each channel measurement  
156 were used to calculate CO<sub>2</sub> fluxes. For calculation of CO<sub>2</sub> emissions, biased, negative CO<sub>2</sub>  
157 fluxes were rejected (<6%).

158

159



## 161 **3 Results**

### 162 *3.1 CO<sub>2</sub> release decreased with progressing number of thaw-freeze periods*

163 CO<sub>2</sub> fluxes during the whole incubation period generally decreased within all treatments  
164 as the number of thaw (Fig. 2) and freeze periods (Fig. 3) proceeds. Treatments of +Si and  
165 +CaSi however, decreased with -57% and -52% much more rapidly from the first to the last  
166 observed thaw period (period with temperature >1°C) compared to the control and +Ca  
167 treatment with -24% and -40%, respectively. The same was observed for the change from the  
168 first to the last observed freeze period (period with temperature <-1°C), were +Si and +CaSi  
169 decreased by -82% and -70%, while CO<sub>2</sub> fluxes of the control and +Ca treatment decreased  
170 by -40% and -60%. As a result, differences between treatments during freeze periods with +Si  
171 being significantly higher diminished during the second freeze period ( $p=0.015$ , compare the  
172 second and the third period) and only significant difference ( $p < 0.01$ ) during thaw periods  
173 between treatments persist.

174 However, despite completely water saturated soil samples, no CH<sub>4</sub> emissions for any of the  
175 treatments were found.

176

### 177 *3.2 Silicon increased and calcium decreased CO<sub>2</sub> fluxes and emissions*

178 CO<sub>2</sub> fluxes generally showed very high variability over time. Therefore, especially the  
179 effects of changing temperatures were not immediately recognizable at a glance (Fig. S1).  
180 However, average CO<sub>2</sub> fluxes during the whole incubation period in the +Si treatment with a  
181 median of 0.055  $\mu\text{mol m}^{-2} \text{s}^{-1}$  were 22% higher and significantly different ( $p=0.01$ , Wilcoxon  
182 test) compared to the control (0.045  $\mu\text{mol m}^{-2} \text{s}^{-1}$ ). In comparison to the +Ca and the +Ca+Si  
183 treatments, which produced CO<sub>2</sub> flux medians of 0.021  $\mu\text{mol m}^{-2} \text{s}^{-1}$  and 0.023  $\mu\text{mol m}^{-2} \text{s}^{-1}$ ,  
184 respectively, the +Si treatment yielded also significantly higher CO<sub>2</sub> fluxes ( $p < 0.01$ , Wilcoxon  
185 test) (Fig. 4a). The same holds true for the CO<sub>2</sub> fluxes from the control treatment, which were

186 also significantly higher ( $p < 0.01$ , Wilcoxon test) compared to the +Ca and the +Ca+Si  
187 treatments. No significant differences in CO<sub>2</sub> fluxes were found between the +Ca and the  
188 +Ca+Si treatment ( $p = 0.015$ ; Wilcoxon test). Daily differences in CO<sub>2</sub> fluxes of the different  
189 treatments compared to control were shown in Figure S1.

190 CO<sub>2</sub> fluxes above +1°C of both the control treatment with a median of 0.043 μmol m<sup>-2</sup>  
191 s<sup>-1</sup> and the +Si treatment with a median of 0.049 μmol m<sup>-2</sup> s<sup>-1</sup> were significantly higher  
192 ( $p < 0.01$ , Wilcoxon test) compared to those of the +Ca with a median of 0.022 μmol m<sup>-2</sup> s<sup>-1</sup>  
193 and the +Ca+Si treatment with a median of 0.025 μmol m<sup>-2</sup> s<sup>-1</sup> (Fig. 4b). Focusing on the CO<sub>2</sub>  
194 fluxes below -1°C we found a strong and significant increase in CO<sub>2</sub> fluxes by 100% in the  
195 +Si treatment with a median of 0.030 μmol m<sup>-2</sup> s<sup>-1</sup> compared to the control treatment with a  
196 median of 0.015 μmol m<sup>-2</sup> s<sup>-1</sup>. No significant difference were found between the control  
197 treatment and both the +Ca treatment with a median of 0.014 μmol m<sup>-2</sup> s<sup>-1</sup> and the +Ca+Si  
198 treatment with a median of 0.016 μmol m<sup>-2</sup> s<sup>-1</sup> (Fig. 4c). For the CO<sub>2</sub> fluxes above +1°C the  
199 pattern was different compared with those fluxes below -1°C.

200 Cumulative CO<sub>2</sub> emissions per treatment during the whole incubation period are shown  
201 in Fig. 5. Similar to average fluxes, the +Si treatment yielded 28% higher cumulative CO<sub>2</sub>  
202 emission (2.44 mg CO<sub>2</sub>-C per sample) when compared to the control treatment (1.90 mg CO<sub>2</sub>-  
203 C sample<sup>-1</sup>). The +Ca and +Ca+Si treatments showed lower cumulative CO<sub>2</sub> emissions (1.13  
204 and 1.47 mg CO<sub>2</sub>-C sample<sup>-1</sup>) compared to the control, with +Ca evidencing the lowest  
205 cumulative CO<sub>2</sub> emissions. Neither of both +Ca and +Ca+Si treatments showed a clear  
206 difference when compared to a proxy for the absence of frost-thaw, represented by the  
207 cumulative CO<sub>2</sub> emission, estimated based on the linear extrapolated, initially measured,  
208 average CO<sub>2</sub> flux of the control treatment at -1°C incubation temperature. Only the +Si  
209 treatment yielded in substantially higher cumulative CO<sub>2</sub> emissions.

210

## 212 **4 Discussion**

213 The main finding of our study is that with each freeze-thaw cycle the CO<sub>2</sub> fluxes from the  
214 Arctic soils decreased, refuting hypothesis (i). We also found pronounced differences between  
215 the tested treatments with Si increasing and Ca decreasing Arctic soil CO<sub>2</sub> fluxes, confirming  
216 hypothesis (ii).

217 Frozen conditions prevent organic matter (OM) from microbial degradation (Mann et al.,  
218 2022) and low temperatures around the freezing point greatly reduce CH<sub>4</sub> emissions (Yvon-  
219 Durocher et al., 2014). This is also a possible explanation for the absence of CH<sub>4</sub> emissions in  
220 our investigations, despite soil samples being completely saturated with water during the  
221 entire experiment. Our data revealed a considerable CO<sub>2</sub> emission below 0°C, especially for  
222 the Si fertilized treatments. This is in line with earlier findings also showing CO<sub>2</sub> emission  
223 from Arctic soil until minus 5°C (Ludwig et al., 2006; Sapronov, 2021; Schimel and Clein,  
224 1996; Wang et al., 2014). Consistent with our data, other studies of Arctic soils also  
225 experienced a decrease in CO<sub>2</sub> release with increasing number of freeze-thaw cycles (Ludwig  
226 et al., 2006; Schimel and Clein, 1996; Wang et al., 2014). This means that the labile organic  
227 carbon in Arctic soils is likely degraded rapidly, once the soil is thawed, needing only few  
228 freeze-thaw cycles to be mineralized and released to the atmosphere.

229 Consequently, higher Arctic temperatures with subsequent increased number of freeze-thaw  
230 cycles per year (oscillation around 0°C) (Henry, 2008) may contribute only to a minor extent  
231 to an increased soil CO<sub>2</sub> release in future, as long as no labile C input by e.g. plants occurs,  
232 since labile C may potentially increases the microbial organic C degradation and subsequent  
233 C release from Arctic soils (Oztas and Fayetorbay, 2003).

234 It is debated in literature how stabile Arctic C is upon soil thaw and the timescale of organic C  
235 degradation in high latitude systems is still unknown (Schuur et al., 2015). Our results

236 indicate that a strong response in CO<sub>2</sub> could take place rapidly after only few thawing cycles,  
237 thus soil thaw could have a direct impact on climate change in the near-future.

238 The effects of Si enhancing CO<sub>2</sub> fluxes from Arctic soils is in line with previous studies on  
239 Greenlandic soils (Schaller et al., 2019) or peatlands (Hömberg et al., 2021; Reithmaier et al.,  
240 2017). This enhanced CO<sub>2</sub> fluxes from Arctic soils by Si may be explained by an increase of  
241 available water (Schaller et al., 2020) without increasing salinity. Another potential  
242 mechanism underlying the enhancing CO<sub>2</sub> fluxes from Arctic soils by Si may be arising from  
243 the mobilization of silicic acid from the ASi (Schaller et al., 2021). Since silicic acid  
244 competes with phosphate for binding at the surfaces of soil particles, previously unavailable  
245 phosphate is potentially mobilized reducing the phosphate limitation for the decomposing  
246 microbes (Hömberg et al., 2020; Schaller et al., 2019). As the strongest effect of +Si treatment  
247 enhancing CO<sub>2</sub> fluxes from Arctic soils was shown for temperatures below 0°C, the Si effect  
248 may have something to do with water availability below 0°C with increased “supercooled”  
249 water content under higher Si concentrations, which has been previously found for increased  
250 silt fractions enhancing the fractions of “supercooled” water at freezing conditions (Schaefer  
251 and Jafarov, 2016). Si in solution was found long time ago to reduce the water freezing point  
252 (Kahlenberg and Lincoln, 1898), which was confirmed recently (Kumar et al., 2019). This  
253 may lead to an increased water availability below 0°C by Si being a potential the reason for  
254 the higher CO<sub>2</sub> fluxes from the Arctic soil below 0°C in the +Si treatment (Fig. 4c) as  
255 microbes need available water.

256 The decrease of the soil CO<sub>2</sub> production rate by Ca is in line with earlier finding (Schaller et  
257 al., 2019; Whittinghill and Hobbie, 2012). This effect of Ca decreasing the soil CO<sub>2</sub>  
258 production rate may be explained by either cation bridging of soil organic matter by Ca ions  
259 (making the organic matter unavailable for microbial decomposition) (Schaller et al., 2019;  
260 Whittinghill and Hobbie, 2012) or by increasing salinity due to Ca addition potentially

261 decreasing activity of microbial decomposer community (Mavi et al., 2012). It was recently  
262 shown that Si may be able to increase and Ca decrease the activity of microbial decomposers  
263 and change the microbial decomposer community structure (Stimmler et al., 2022).  
264 We show that both Si and Ca concentrations in Arctic soils are a main controls on Arctic soil  
265 CO<sub>2</sub> release, with Si increasing soil CO<sub>2</sub> release especially when temperatures are below 0°C.  
266 High-Arctic permafrost soils store vast amounts of Si and Ca (Alfredsson et al., 2016;  
267 Stimmler et al., in revision; Walker et al., 2001), which could be released upon thaw. These  
268 feedbacks which affect soil organic matter stabilization in Arctic soil (potentially by Ca) are  
269 poorly understood and such effects of stabilization of organic matter by Ca potentially  
270 decreasing soil respiration and/ or a mobilization of nutrient like phosphate by Si potentially  
271 increasing soil respiration are not taken into account in present global-scale assessments of the  
272 Arctic carbon budget (Canadell et al., 2021). If our findings regarding soil respiration effects  
273 of Si and Ca on Arctic soil organic matter turn out to be true on larger scales, they could  
274 provide an important constraint on soil CO<sub>2</sub> emissions upon soil thaw, as well as on the  
275 greenhouse gas budget of high latitudes. We thus call for work improving understanding on  
276 Ca and Si feedbacks on carbon fluxes, as well as for increased consideration of factors that  
277 affect the stability of Arctic soil carbon in wide-scale assessments.

278 A first step towards this is the development of an experimental design for the studies, which  
279 accurately captures the real conditions on thawed Arctic soils. An important impetus for this  
280 is the small post-thaw CO<sub>2</sub> pulse in our studies, which further decreased with proceeding  
281 freeze-thaw cycles. While a strong CO<sub>2</sub> pulse occurred in three of the studies that looked at  
282 the effect of freeze-thaw cycles on Arctic soils (Sapronov, 2021; Schimel and Clein, 1996;  
283 Wang et al., 2014), it was also absent in Ludwig et al. (2006). Apparently, this was because, in  
284 agreement with Ludwig et al. (2006, we had only slowly changed the temperature during the  
285 transition between freeze-thaw or vice versa, as actually occurring under natural conditions in

286 Arctic soils. In other words, the CO<sub>2</sub> pulse observed by most other studies may be a result of  
287 an abrupt transition between temperature phases does not reflect the real situation on thawing  
288 Arctic soils. However, it is possible that the very high-frequency measurement of CO<sub>2</sub> fluxes  
289 used by our study and the study of Ludwig et al. (2006 simply made visible that CO<sub>2</sub> fluxes in  
290 Arctic soils fluctuate much more than previously perceived. The same holds true for the  
291 generalizability of the conclusions obtained in incubation experiments with small amounts of  
292 soil to the reduction of CO<sub>2</sub> release with increasing number of freeze-thaw cycles. At least, it  
293 cannot be excluded that factors such as the presence of temperature and matter gradients in  
294 the soil profile, soil movements due to cryoturbation, and the diverse activities of plants alter  
295 the effects of freeze-thaw cycles on CO<sub>2</sub> release in the field (Mauritz et al., 2021; Olid et al.,  
296 2020; Treat et al., 2021). Therefore, the focus of future investigations should be to clarify  
297 exactly this.

298

300  
301  
302  
303  
304  
305  
306  
307  
308  
309  
310  
311  
312  
313  
314  
315  
316  
317  
318  
319  
320  
321  
322  
323  
324

## References

- Alfredsson H, Clymans W, Hugelius G, Kuhry P, Conley DJ. Estimated storage of amorphous silica (ASi) in soils of the circum-Arctic tundra region. *Glob. Biogeochem. Cycle* 2016; 30: 479–500.
- Anderson TR, Hawkins E, Jones PD. CO<sub>2</sub>, the greenhouse effect and global warming: from the pioneering work of Arrhenius and Callendar to today's Earth System Models. *Endeavour* 2016; 40: 178-187.
- Canadell JG, Monteiro PM, Costa MH, Da Cunha LC, Cox PM, Alexey V, Henson S, Ishii M, Jaccard S, Koven C, Lohila A, Patra P, Piao S, Rogelj J, Syampungani S, Zaehle S, Zickfeld K. Global carbon and other biogeochemical cycles and feedbacks. In: Masson-Delmotte V, Zhai P, Pirani A, Connors S, Péan C, Berger S, Caud N, Chen Y, Goldfarb L, Gomis M, Huang M, Leitzell K, Lonnoy E, Matthews J, Maycock T, Waterfield T, Yelekçi O, Yu R, Zhou B, editors. *Climate Change 2021: The Physical Science Basis. Contribution of Working Group I to the Sixth Assessment Report of the Intergovernmental Panel on Climate Change*. Cambridge University Press, Cambridge, United Kingdom, 2021, pp. 673–816.
- Göckede M, Kittler F, Kwon MJ, Burjack I, Heimann M, Kolle O, Zimov N, Zimov S. Shifted energy fluxes, increased Bowen ratios, and reduced thaw depths linked with drainage-induced changes in permafrost ecosystem structure. *The Cryosphere* 2017; 11: 2975-2996.
- Göckede M, Kwon MJ, Kittler F, Heimann M, Zimov N, Zimov S. Negative feedback processes following drainage slow down permafrost degradation. *Glob. Change Biol.* 2019; 25: 3254-3266.

325 Grogan P, Michelsen A, Ambus P, Jonasson S. Freeze–thaw regime effects on carbon and  
326 nitrogen dynamics in sub-arctic heath tundra mesocosms. *Soil Biology and*  
327 *Biochemistry* 2004; 36: 641-654.

328 Henry HA. Soil freeze–thaw cycle experiments: trends, methodological weaknesses and  
329 suggested improvements. *Soil Biology and Biochemistry* 2007; 39: 977-986.

330 Henry HA. Climate change and soil freezing dynamics: historical trends and projected  
331 changes. *Climatic Change* 2008; 87: 421-434.

332 Heslop JK, Winkel M, Walter Anthony KM, Spencer RGM, Podgorski DC, Zito P, Kholodov  
333 A, Zhang M, Liebner S. Increasing Organic Carbon Biolability With Depth in Yedoma  
334 Permafrost: Ramifications for Future Climate Change. *Journal of Geophysical*  
335 *Research: Biogeosciences* 2019; 124: 2021-2038.

336 Hömberg A, Broder T, Knorr K-H, Schaller J. Divergent effect of silicon on greenhouse gas  
337 production from reduced and oxidized peat organic matter. *Geoderma* 2021; 386:  
338 114916.

339 Hömberg A, Obst M, Knorr K-H, Kalbitz K, Schaller J. Increased silicon concentration in fen  
340 peat leads to a release of iron and phosphate and changes in the composition of  
341 dissolved organic matter. *Geoderma* 2020; 374: 114422.

342 Hugelius G, Strauss J, Zubrzycki S, Harden JW, Schuur E, Ping C-L, Schirrmeister L, Grosse  
343 G, Michaelson GJ, Koven CD. Estimated stocks of circumpolar permafrost carbon  
344 with quantified uncertainty ranges and identified data gaps. *Biogeosciences* 2014; 11:  
345 6573-6593.

346 Kahlenberg L, Lincoln A. Solutions of silicates of the alkalies. *Journal of Physical Chemistry*  
347 1898; 2: 77-90.



348 Kim DG, Vargas R, Bond-Lamberty B, Turetsky MR. Effects of soil rewetting and thawing  
349 on soil gas fluxes: a review of current literature and suggestions for future research.  
350 *Biogeosciences* 2012; 9: 2459-2483.

351 Kumar A, Marcolli C, Peter T. Ice nucleation activity of silicates and aluminosilicates in pure  
352 water and aqueous solutions—Part 2: Quartz and amorphous silica. *Atmospheric*  
353 *Chemistry and Physics* 2019; 19: 6035-6058.

354 Kurganova I, Teepe R, Loftfield N. Influence of freeze-thaw events on carbon dioxide  
355 emission from soils at different moisture and land use. *Carbon balance and*  
356 *management* 2007; 2: 1-9.

357 Lipson DA, Schmidt SK, Monson RK. Carbon availability and temperature control the post-  
358 snowmelt decline in alpine soil microbial biomass. *Soil Biology and Biochemistry*  
359 2000; 32: 441-448.

360 Livingston G, Hutchinson G. Enclosure-based measurement of trace gas exchange:  
361 applications and sources of error. *Biogenic trace gases: measuring emissions from soil*  
362 *and water* 1995; 51: 14-51.

363 Loiko SV, Pokrovsky OS, Raudina TV, Lim A, Kolesnichenko LG, Shirokova LS, Vorobyev  
364 SN, Kirpotin SN. Abrupt permafrost collapse enhances organic carbon, CO<sub>2</sub>, nutrient  
365 and metal release into surface waters. *Chemical Geology* 2017; 471: 153-165.

366 Ludwig B, Teepe R, Lopes de Gerenyu V, Flessa H. CO<sub>2</sub> and N<sub>2</sub>O emissions from gleyic  
367 soils in the Russian tundra and a German forest during freeze–thaw periods—a  
368 microcosm study. *Soil Biology and Biochemistry* 2006; 38: 3516-3519.

369 Mann PJ, Strauss J, Palmtag J, Dowdy K, Ogneva O, Fuchs M, Bedington M, Torres R,  
370 Polimene L, Overduin P. Degrading permafrost river catchments and their impact on  
371 Arctic Ocean nearshore processes. *Ambio* 2022; 51: 439-455.

372 Mauritz M, Pegoraro E, Ogle K, Ebert C, Schuur EAG. Investigating Thaw and Plant  
373 Productivity Constraints on Old Soil Carbon Respiration From Permafrost. *Journal of*  
374 *Geophysical Research: Biogeosciences* 2021; 126.

375 Mavi MS, Marschner P, Chittleborough DJ, Cox JW, Sanderman J. Salinity and sodicity  
376 affect soil respiration and dissolved organic matter dynamics differentially in soils  
377 varying in texture. *Soil Biology and Biochemistry* 2012; 45: 8-13.

378 Mueller CW, Rethemeyer J, Kao-Kniffin J, Löppmann S, Hinkel KM, G. Bockheim J. Large  
379 amounts of labile organic carbon in permafrost soils of northern Alaska. *Glob.*  
380 *Change Biol.* 2015; 21: 2804-2817.

381 Olid C, Klaminder J, Monteux S, Johansson M, Dorrepaal E. Decade of experimental  
382 permafrost thaw reduces turnover of young carbon and increases losses of old carbon,  
383 without affecting the net carbon balance. *Glob Chang Biol* 2020; 26: 5886-5898.

384 Ouyang W, Lai X, Li X, Liu H, Lin C, Hao F. Soil respiration and carbon loss relationship  
385 with temperature and land use conversion in freeze–thaw agricultural area. *Sci. Total*  
386 *Environ.* 2015; 533: 215-222.

387 Oztas T, Fayetorbay F. Effect of freezing and thawing processes on soil aggregate stability.  
388 *Catena* 2003; 52: 1-8.

389 Payandi-Rolland D, Shirokova LS, Nakhle P, Tesfa M, Abdou A, Causserand C, Lartiges B,  
390 Rols J-L, Guérin F, Bénézet P, Pokrovsky OS. Aerobic release and biodegradation of  
391 dissolved organic matter from frozen peat: Effects of temperature and heterotrophic  
392 bacteria. *Chemical Geology* 2020; 536.

393 Reithmaier GMS, Knorr KH, Arnhold S, Planer-Friedrich B, Schaller J. Enhanced silicon  
394 availability leads to increased methane production, nutrient and toxicant mobility in  
395 peatlands. *Scientific Reports* 2017; 7: 8728.

396 Rillig MC, Hoffmann M, Lehmann A, Liang Y, Lück M, Augustin J. Microplastic fibers  
397 affect dynamics and intensity of CO<sub>2</sub> and N<sub>2</sub>O fluxes from soil differently.  
398 *Microplastics and Nanoplastics* 2021; 1: 1-11.

399 Sapronov DV. The CO<sub>2</sub> Emission during Laboratory Freezing-Thawing of Soils from  
400 Various Natural Zones of Russia. *Eurasian Soil Science* 2021; 54: 1196-1205.

401 Schaefer K, Jafarov E. A parameterization of respiration in frozen soils based on substrate  
402 availability. *Biogeosciences* 2016; 13: 1991-2001.

403 Schaller J, Cramer A, Carminati A, Zarebanadkouki M. Biogenic amorphous silica as main  
404 driver for plant available water in soils. *Scientific Reports* 2020; 10: 2424.

405 Schaller J, Fauchere S, Joss H, Obst M, Goeckede M, Planer-Friedrich B, Peiffer S, Gilfedder  
406 B, Elberling B. Silicon increases the phosphorus availability of Arctic soils. *Scientific*  
407 *Reports* 2019; 9: 449.

408 Schaller J, Puppe D, Kaczorek D, Ellerbrock R, Sommer M. Silicon Cycling in Soils  
409 Revisited. *Plants* 2021; 10: 295.

410 Schimel JP, Clein JS. Microbial response to freeze-thaw cycles in tundra and taiga soils. *Soil*  
411 *Biol. Biochem.* 1996; 28: 1061-1066.

412 Schuur E, McGuire A, Schädel C, Grosse G, Harden J, Hayes D, Hugelius G, Koven C,  
413 Kuhry P, Lawrence D, Natali S, Olefeldt D, Romanovsky V, Schaefer K, Turetsky M,  
414 Treat C, Vonk V. Climate change and the permafrost carbon feedback. *Nature* 2015;  
415 520: 171-179.

416 Skogland T, Lomeland S, Goksøyr J. Respiratory burst after freezing and thawing of soil:  
417 Experiments with soil bacteria. *Soil Biology and Biochemistry* 1988; 20: 851-856.

418 Stimmler P, Goeckede M, Elberling B, Natali S, Kuhry P, Perron N, Lacroix F, Hugelius G,  
419 Sonnentag O, Strauss J, Minions C, Sommer M, Schaller J. Pan-Arctic soil element  
420 bioavailability estimations. *Earth System Science Data* in revision.

421 Stimmler P, Priemé A, Elberling B, Goeckede M, Schaller J. Arctic soil respiration and  
422 microbial community structure driven by silicon and calcium. *Sci. Total Environ.*  
423 2022; 838: 156152.

424 Stocker T, Qin D, Plattner G-K, Tignor M, Allen SK, Boschung J, Nauels A, Xia Y, Bex V,  
425 Midgley PM. *Climate change 2013: The physical science basis: Cambridge University*  
426 *Press Cambridge, UK, and New York, 2014.*

427 Treat CC, Jones MC, Alder J, Sannel ABK, Camill P, Frohking S. Predicted Vulnerability of  
428 Carbon in Permafrost Peatlands With Future Climate Change and Permafrost Thaw in  
429 Western Canada. *Journal of Geophysical Research: Biogeosciences* 2021; 126.

430 Walker D, Bockheim J, Chapin F, Eugster W, Nelson F, Ping C. Calcium-rich tundra,  
431 wildlife, and the “Mammoth Steppe”. *Quaternary Science Reviews* 2001; 20: 149-163.

432 Wang J, Song C, Hou A, Wang L. CO<sub>2</sub> emissions from soils of different depths of a  
433 permafrost peatland, Northeast China: response to simulated freezing–thawing cycles.  
434 *Journal of Plant Nutrition and Soil Science* 2014; 177: 524-531.

435 Whittinghill KA, Hobbie SE. Effects of pH and calcium on soil organic matter dynamics in  
436 Alaskan tundra. *Biogeochemistry* 2012; 111: 569-581.

437 Yvon-Durocher G, Allen AP, Bastviken D, Conrad R, Gudasz C, St-Pierre A, Thanh-Duc N,  
438 del Giorgio PA. Methane fluxes show consistent temperature dependence across  
439 microbial to ecosystem scales. *Nature* 2014; 507: 488-91.

440 Zhang J, Hong J, Wei D, Wang X. Severe freezing increases soil respiration during the  
441 thawing period: A meta-analysis. *European Journal of Soil Science* 2021; 73.

442

443

444 **Acknowledgments**

445 Special thanks to Mathias Lück (ZALF) for help with measurement and experimental setup.

446 The work was funded by the German Research Foundation (DFG), grant number

447 SCHA 1822/12-1 to Jörg Schaller.

448

449

450 **Author contributions:** JS, PS and MH designed the study. MG provided the soil. MH did the

451 measurements. All authors discussed the results and contributed substantially to the

452 manuscript.

453

454 **Competing interests:** The authors declare no competing interests.

455

457 **Tables**

458 Tab. 1: average measured CO<sub>2</sub>, CH<sub>4</sub> and N<sub>2</sub>O fluxes for the different treatments during the  
 459 repetitive freeze-thaw-cycle

Period	Treatment	Temp.	CO <sub>2</sub>	CH <sub>4</sub>	N <sub>2</sub> O
		°C			
<b>1<sup>st</sup> thaw</b>	control	4.0	52	-0.01	0.01
	+Ca	4.0	25	-0.02	<0.00
	+Si	4.0	76	0.02	<0.00
	+Ca+Si	4.0	35	0.01	<0.00
<b>1<sup>st</sup> freeze</b>	control	-3.2	21	<0.00	0.01
	+Ca	-3.5	34	-0.02	0.01
	+Si	-3.4	61	0.02	0.03
	+Ca+Si	-3.2	51	0.02	0.01
<b>2<sup>nd</sup> thaw</b>	control	3.5	57	-0.01	<0.00
	+Ca	3.4	31	0.01	<0.00
	+Si	3.5	49	<0.00	<0.00
	+Ca+Si	3.5	33	<0.00	<0.00
<b>2<sup>nd</sup> freeze</b>	control	-3.6	9	<0.00	0.01
	+Ca	-3.8	13	<0.00	-0.01
	+Si	-3.8	16	<0.00	<0.00
	+Ca+Si	-3.5	6	<0.00	0.01
<b>3<sup>rd</sup> thaw</b>	control	3.4	36	<0.00	<0.00
	+Ca	3.5	17	0.01	<0.00
	+Si	3.6	26	0.01	-0.01
	+Ca+Si	3.5	8	-0.01	-0.01

460

461

462

463

464

465

466

467

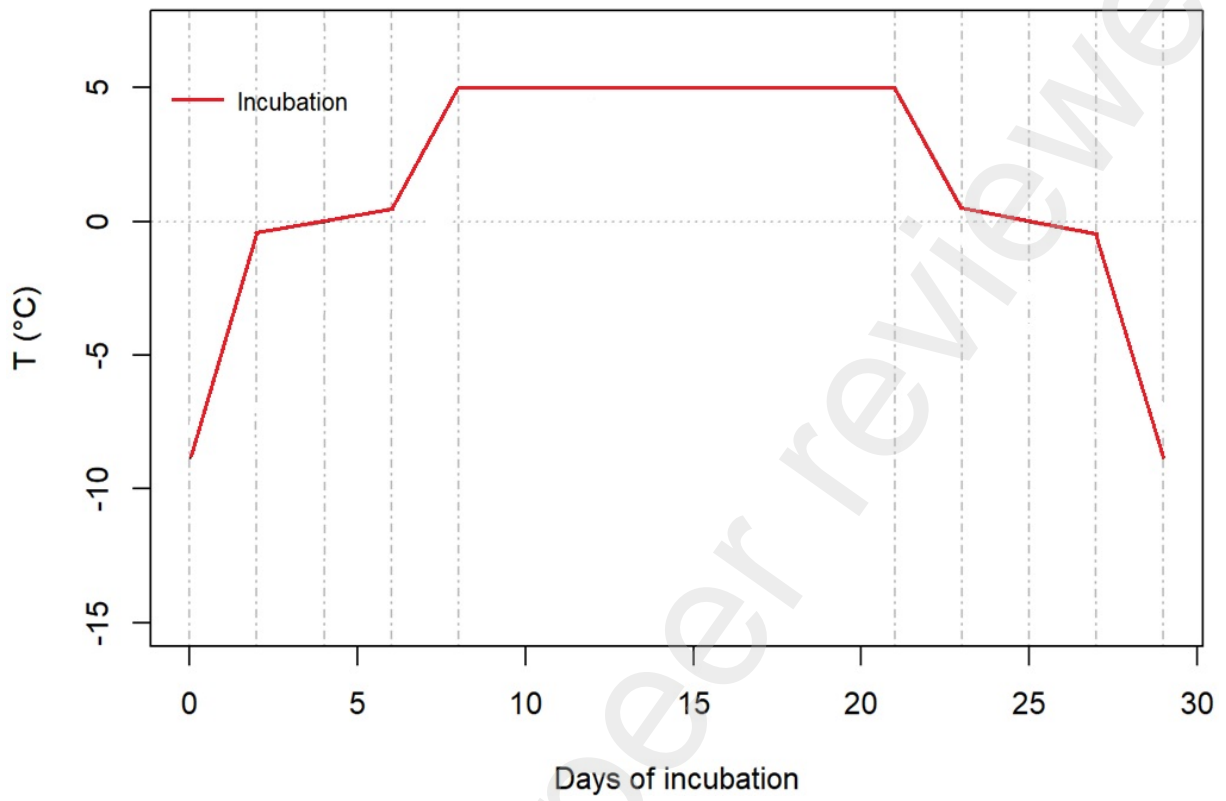
468

469

470

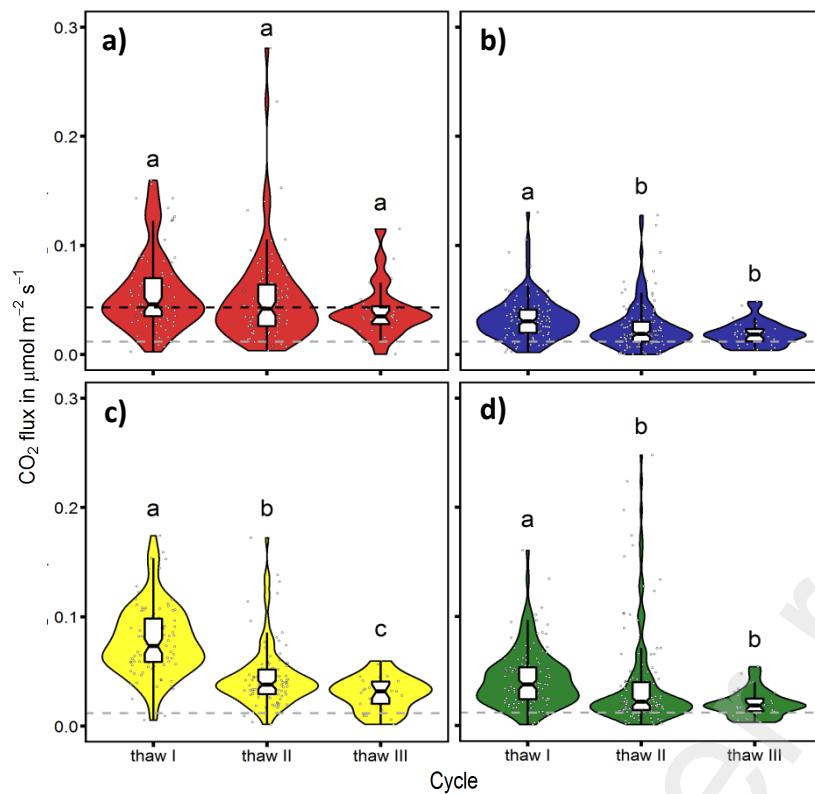
471 **Figures**

472



473

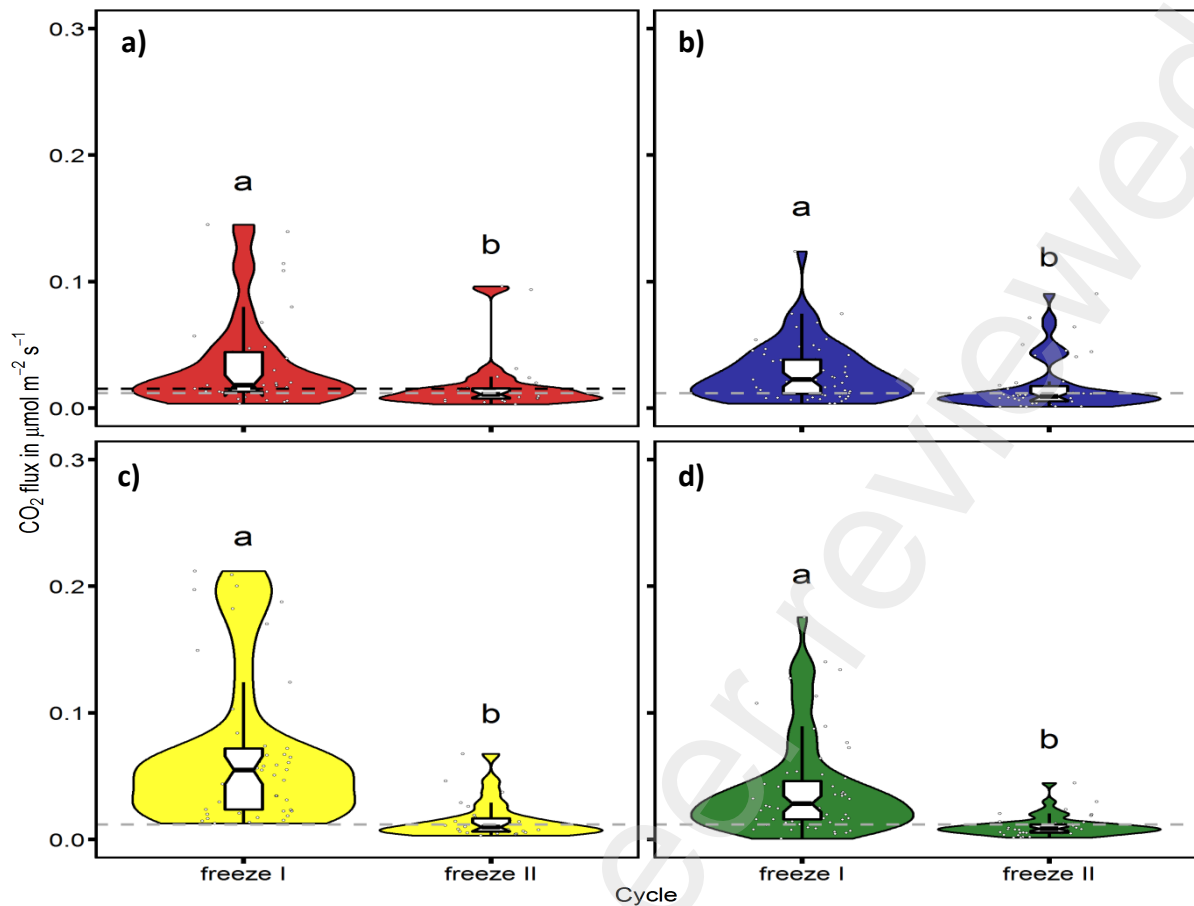
474 Fig. 1: Schematic representation of the time schedule and temperature regime of one freeze-  
475 thaw-cycle simulated during the incubation experiment



476

477 Fig. 2: Measured CO<sub>2</sub> fluxes of the a) control, b) +Ca, c) +Si and d) +Si+Ca treatment during  
 478 the first, second and third thaw period (defined as incubation temperature >+1°C following  
 479 freeze) within the incubation period. The dashed black horizontal line indicated the median  
 480 CO<sub>2</sub> flux of the control treatment (a), the dashed gray horizontal line the initially measured,  
 481 average CO<sub>2</sub> flux of the control treatment at -1°C. Different letters indicate significant  
 482 ( $p < 0.05$ ) difference between CO<sub>2</sub> fluxes of the different thawing periods.





484

485 Fig. 3: Measured CO<sub>2</sub> fluxes of the of the a) control, b) +Ca, c) +Si and d) +Si+Ca treatment  
 486 during the first and second freeze period (defined as incubation temperature  $< -1^{\circ}\text{C}$  following  
 487 thaw) within the incubation period. The dashed black horizontal line indicates the median  
 488 CO<sub>2</sub> flux of the control treatment (a). The dashed gray horizontal line indicates the initially  
 489 measured, average CO<sub>2</sub> flux of the control treatment at  $-1^{\circ}\text{C}$ . Different letters indicate  
 490 significant ( $p < 0.05$ ) difference between CO<sub>2</sub> fluxes of the different freeze cycles.

491

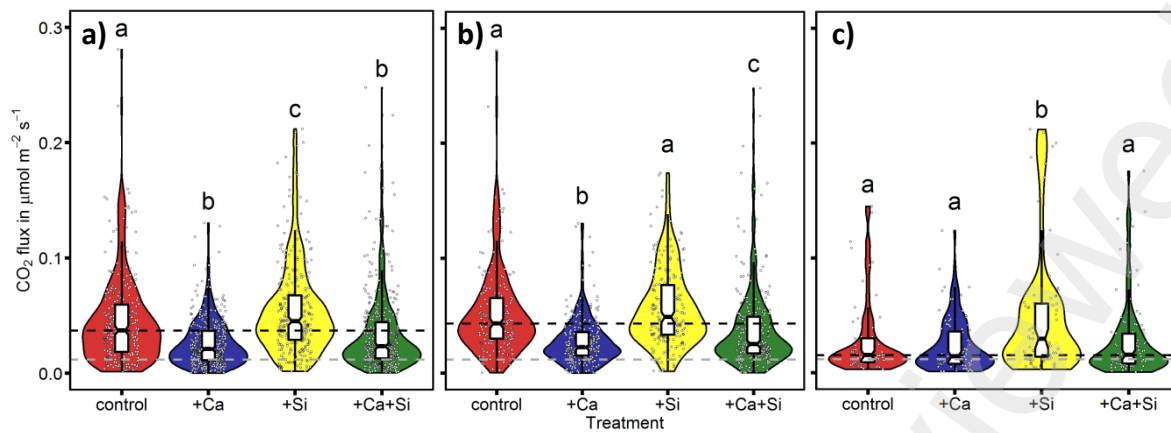
492

493

494

495

496



497

498 Fig. 4: Measured CO<sub>2</sub> fluxes of the a) different treatments for the entire incubation period; b)  
 499 shows measured CO<sub>2</sub> fluxes for the different treatments when incubation temperature was  
 500 above +1°C and c) shows measured CO<sub>2</sub> fluxes for the different treatments when incubation  
 501 temperature was below -1°C. The dashed black horizontal line indicated the median CO<sub>2</sub> flux  
 502 of the control treatment, the dashed gray horizontal line the initially measured, average CO<sub>2</sub>  
 503 flux of the control treatment at -1°C incubation temperature. Different letters indicate  
 504 significant ( $p < 0.05$ ) differences between CO<sub>2</sub> fluxes of the different treatments.

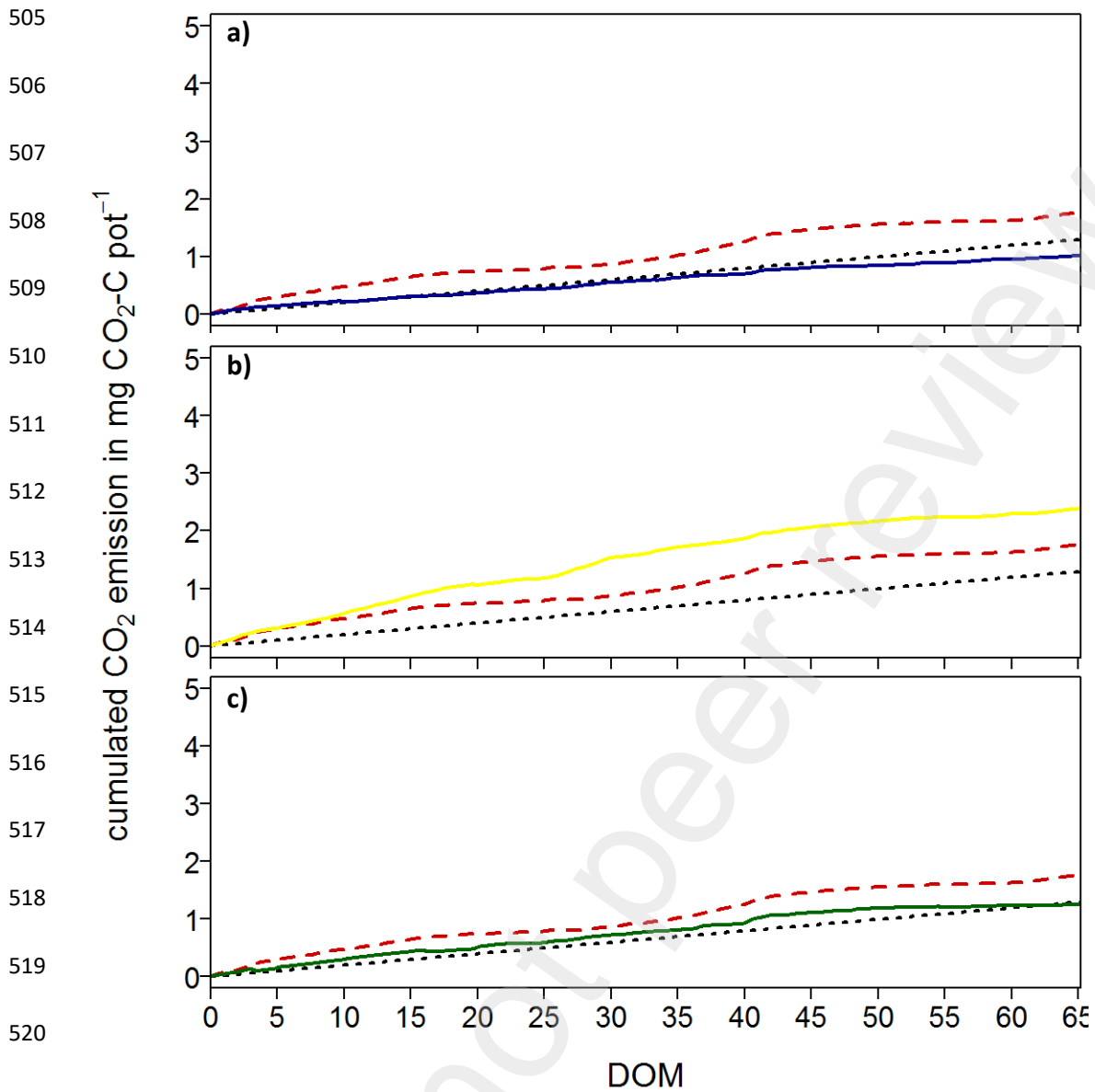


Fig. 5: Cumulative CO<sub>2</sub> emissions over the whole incubation period for the a) +Ca, b) +Si and c) +Ca+Si treatment. The dashed, red line represents the cumulative CO<sub>2</sub> emission of the control treatment. The dotted black line indicated the cumulative CO<sub>2</sub> flux based on the initially measured, average CO<sub>2</sub> flux of the control treatment at -1°C.